A&A 413, 1183–1189 (2004)
DOI: 10.1051/0004-6361:20031548

Astronomy & Astrophysics

DOT tomography of the solar atmosphere

I. Telescope summary and program definition

R. J. Rutten[1,2], R. H. Hammerschlag[1], F. C. M. Bettonvil[1,3], P. Sütterlin[1], and A. G. de Wijn[1]

[1] Sterrekundig Instituut, Utrecht University, Postbus 80 000, 3508 TA Utrecht, The Netherlands
e-mail: R.J.Rutten; R.H.Hammerschlag; F.C.M.Bettonvil; P.Suetterlin; A.G.deWijn@astro.uu.nl
[2] Institute of Theoretical Astrophysics, Oslo University, PO Box 1029 Blindern, 0315 Oslo, Norway
[3] ASTRON/NFRA, Postbus 2, 7990 AA Dwingeloo, The Netherlands

Received 28 July 2003 / Accepted 29 September 2003

Abstract. The Dutch Open Telescope (DOT) on La Palma is an innovative optical solar telescope capable of reaching 0.2 arcsec angular resolution over extended durations. The DOT presently progresses from technology testbed to a stable science configuration providing multi-wavelength imaging and multi-camera speckle data acquisition for tomographic mapping of the solar atmosphere. Large-volume speckle processing will soon enable frequent usage and community-wide time allocation, in particular for tandem operation with other solar telescopes pursuing spectropolarimetry and EUV imaging. We summarize the DOT hardware and software in the context of this increasing availability and outline the corresponding "open-DOT" program.

Key words. telescopes – techniques: image processing – Sun: photosphere – Sun: chromosphere

1. Introduction

The Dutch Open Telescope (DOT) is an innovative optical solar telescope at the Roque de los Muchachos Observatory on La Palma (Canary Islands). We describe its design, construction, instrumentation, data processing and data products in preparation for DOT common-user and service-mode deployment. Our aim is to inform prospective DOT users of the telescope's capabilities for targeting the structure and dynamics of magnetic phenomena throughout the solar atmosphere, in particular through combination with optical and infrared spectropolarimetry at other groundbased solar telescopes and with EUV imaging from space platforms. We plan to "open up" the DOT for frequent partnership in such multi-telescope campaigns in 2004.

Historically, the DOT stems from the extensive European site test campaigns conducted by the Joint Organisation for Solar Observations (JOSO) during the 1970s. They were described in numerous JOSO reports and summarized by Brandt & Righini (1985). They inspired C. Zwaan[1], chairman of JOSO's site testing Working Group, to formulate the concept of a wind-swept open telescope on a non-blocking open pedestal to minimize telescope seeing. He convinced Hammerschlag to design and build such a telescope. The DOT was eventually completed, and installed during 1996–1997 close to the building of the Swedish solar telescope (then the Swedish Vacuum Solar Telescope SVST, now the Swedish 1-m Solar Telescope SST) from which the DOT is operated. The superb initial DOT movie sequences demonstrated the open design as a viable concept to build solar telescopes with larger aperture than the 1-m limit imposed by entrance windows or objective lenses for evacuated telescopes.

The DOT's long-term observing strategy was then defined, namely to combine multi-diagnostic imaging with consistent speckle reconstruction. The background is that the DOT does not offer an image laboratory for flexible instrument setup but instead requires stable instrumentation in the out-of-reach telescope top, with wavefront restoration preferably applied post-detection. Over the past years the instrumentation concepts were tested extensively, an elaborate multi-wavelength post-focus re-imaging system has been developed, and multi-channel speckle-burst data acquisition has been implemented. More detail is given in conference proceedings (Hammerschlag 1981, 1983; Hammerschlag & Bettonvil 1998; Rutten 1999; Sütterlin et al. 2001a; Rutten et al. 2001a; Bettonvil et al. 2003; Hammerschlag et al. 2003), in Rutten (2003), and on the DOT website[2] which also furnishes DOT photographs and most speckle-restored DOT movies taken so far. Example images from the DOT are shown in Fig. 1. Science results from

Send offprint requests to: R. J. Rutten,
e-mail: R.J.Rutten@astro.uu.nl

[1] We dedicate this paper to Cornelis Zwaan (1928–1999) for his role as DOT instigator and for being a leading and inspiring scientist as well as nestor to the first two authors.

[2] http://dot.astro.uu.nl/

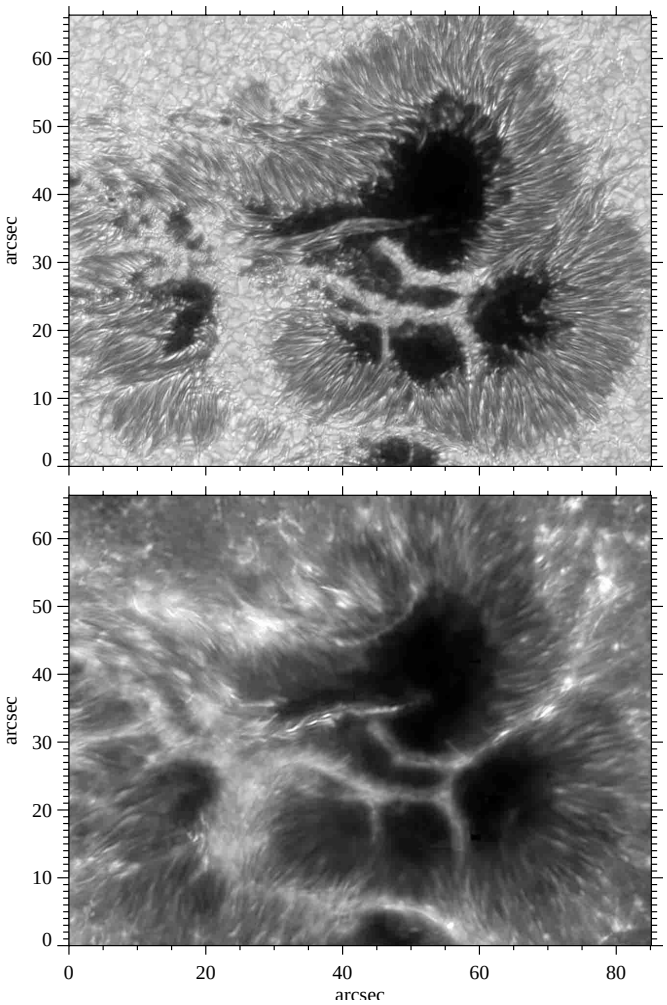

Fig. 1. Simultaneous DOT images of active region AR10349 taken on May 1, 2003 at 13:38 UT. Upper panel: G band (deep photosphere). Lower panel: Ca II H (low chromosphere). Each speckle burst consisted of 100 frames with 0.8 ms and 10 ms exposure, respectively, taken at 6 f/s frame rate with synchronous exposure starts. The field of view was tessellated into 980 isoplanatic subfields which were independently speckle-reconstructed and re-merged. The Fried parameter was r_0 = 7.6 cm and r_0 = 6.0 cm, respectively.

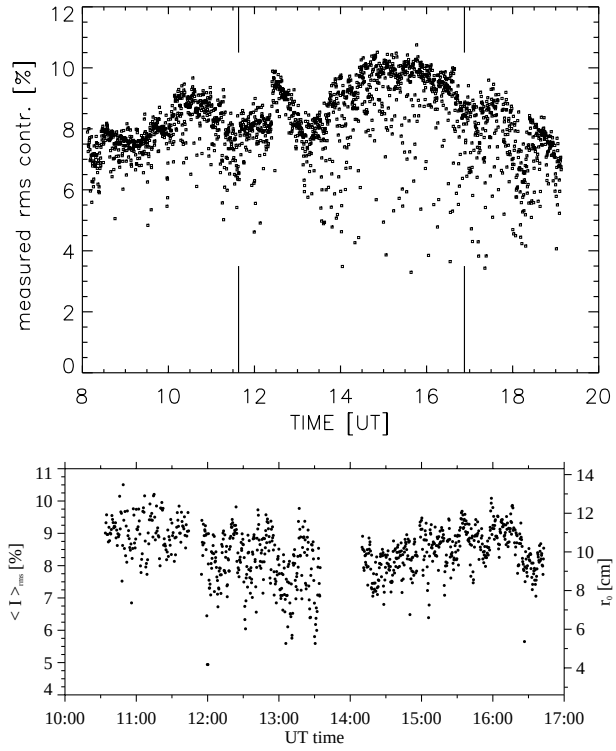

Fig. 2. Examples of diurnal seeing variation at La Palma. Upper plot: granulation contrast during the famous Brandt-Simon 11-hour sequence taken on June 7, 1993 with digital frame selection at the SVST (Simon et al. 1994; figure from Hoekzema et al. 1998). Lower plot: granulation contrast (left) and Fried parameter (right) during three sequences taken with the initial DOT video camera on September 20, 1999. The first, until 11:45, was speckle-reconstructed into a sunspot movie which became the February 23, 2000 "Astronomy Picture of the Day". The other two sequences used frame selection, with conversion of contrast into Fried parameter based on the first sequence. The granulation contrasts are not directly comparable between the two plots because the wavelengths and straylight values differ.

the test phase are presented by Sütterlin (2001), Sobotka & Sütterlin (2001), Balthasar et al. (2001), Nisenson et al. (2003) and Rouppe van der Voort et al. (2003).

The DOT now becomes ready to take on its envisaged role of high-resolution tomographer. It will provide multi-wavelength image and Dopplergram sequences sampling the photosphere and chromosphere across a wide height range (Sect. 4), often at high angular resolution (nearing the 0.2 arcsec diffraction limit already at fair seeing), at reasonably fast cadence (about 20 s), over rather wide fields (about 90×60 arcsec^2), and over rather long durations (up to eight hours when good seeing persists).

These capabilities make the DOT a "tomographic" moviemaker catering to a wide range of solar-physics interests. Important DOT movie characteristics are their homogeneous resolution across the whole field, sustained quality over long durations, co-spatiality, and synchronicity. Tomographic DOT movies will constitute a groundbased optical counterpart to TRACE's EUV movies, will represent precursors to Solar-B's optical image sequences well before this mission orbits, and will be complementary to efforts elsewhere concentrating on adaptive-optics spectropolarimetry.

2. Site characteristics

The Roque de los Muchachos site on La Palma is well-known to deliver extraordinary seeing quality not only to nighttime astronomy but also in solar observing. Nevertheless, there are no quantitative daytime statistics readily available except for the 1979 German campaign (Brandt & Wöhl 1982). The SVST experience has been that superb seeing occurs fairly frequently and may last the whole day (Fig. 2), an unusual characteristic for mountain sites exposed to diurnal solar heating (Lui & Beckers 2001) and a very important asset for solar research requiring long-duration dynamics monitoring (the Brandt–Simon granulation sequence of Fig. 2 generated over a dozen research papers). This favorable condition results from the strong oceanic trade winds, blowing upslope from northern directions, which also flush our telescope. In addition, La Palma's southern

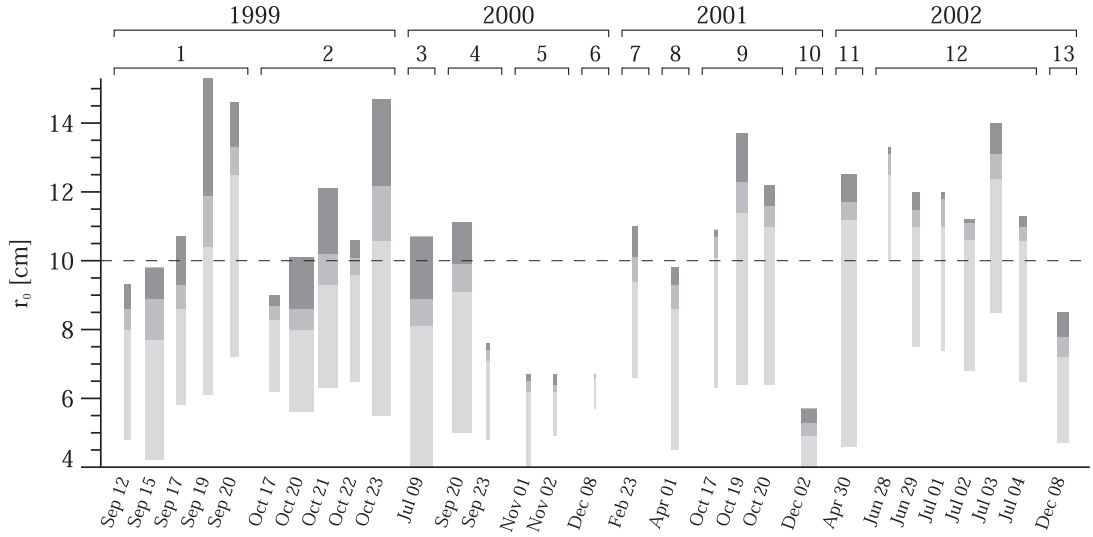

Fig. 3. Fried parameter r_0 during thirteen DOT campaigns. They typically lasted two weeks but only a few days were devoted to science observing. Each bar represents a fully processed speckle sequence, providing quantitative r_0 estimates per speckle burst. The top of each bar specifies r_0 for the best burst, the upper contrast change specifies the mean value for the best 10% of the bursts, the lower the mean of the best 30%. The bottom of each bar represents the worst value but this is insignificant when runs are continued into bad seeing. The bar widths show the sequence durations. The longest (October 20, 1999) lasted 200 min. Durations up to eight hours will be feasible with the new DOT speckle system (Sect. 5).

location well below the jet-stream belt seems to bring favorable high-altitude seeing.

More information is expected from the ongoing ATST site survey (`http://atst.nso.edu/site/`). An older solar scintillation monitor from the preceding CLEAR survey (Beckers & Rutten 1998) on the DOT platform is a reliable low-altitude seeing indicator for both the DOT and the SST.

Figure 3 summarizes our own experience during the DOT test phase. It illustrates that *(i)* – the DOT has been exploited only infrequently so far (being severely limited by the speckle processing, see Sect. 5); *(ii)* – although many campaigns were outside the best-seeing season, good sequences where obtained in nearly all campaigns; *(iii)* – restriction to superb seeing ($r_0 > 10$ cm during 1/3 of the time) passes 1/3 of these sequences, with a good chance of getting at least one per two-week campaign. This is a rather strict criterion since seeing with $r_0 \approx 7$ cm already produces nearly diffraction-limited (0.2 arcsec) speckle reconstructions. For example, the December 8, 2002 sequences (the first tomographic ones with synchronous G-band and Ca II H recording, available on the DOT website) had seeing below the $r_0 = 10$ cm line in Fig. 3 but are good enough to be analyzed in the next paper of this series.

3. Tower, telescope, canopy

The principal guideline in DOT design and construction has been to achieve high pointing stability in the face of openness and considerable wind buffeting. The 15-m high open tower consists of four vertical triangles of slender (24.5-cm diameter) steel tubes supporting an open-mesh telescope platform stiffened by a downward framework (Fig. 4). The four-triangle geometry diminishes platform tilts due to wind loads. Tube eigenfrequency (6 Hz) excitation by wind vorticity is reduced through a combination of rubber dampers and frequency-shifting connectors. More detail is given in Hammerschlag (1973) and Hammerschlag et al. (2003).

The telescope mount is a massive parallactic fork resting on three of the four tower-triangle tops (Fig. 4). Extreme rigidity has been achieved through careful engineering, such as the development of large self-aligning gear trains which maintain line contact between their teeth, and the application of low-load driving to avoid nonlinear stick-slip at slow speeds (Hammerschlag 1983). Pairs of brushless servo motors drive the hour-angle and declination "axes" (actually heavy wheels) in tandem push-pull configurations, with role reversal at local noon.

A separate off-set whole-disk guider telescope with a video camera and frame grabber feeds disk-center position corrections at 5 Hz rate, resulting in sub-arcsecond pointing precision. A software model compensates for differential solar rotation and diurnal flexure of the guider mount.

The primary mirror is parabolic with diameter $D = 450$ mm and focal length $f = 200$ cm. It is made of aluminized Cervit with a protective quartz coating. The outer 6 mm are of lower quality and are stopped off in a secondary pupil plane. The primary is mounted with 3 radial supports of its central hole and 9 cantilevered supports distributed over its backside that exert non-radial forces only.

The telescope top houses the primary-focus field stop, reimaging and multi-wavelength optics, narrow-band filters, and the CCD cameras. It is supported by heavy steel tubes in triangular geometry similar to the tower, but with large stiffness against translational perturbations.

Lab-based mirror interferometry served to construct precise diode-laser and mechanical focus alignment markers which were used to ensure that the secondary DOT optics is precisely

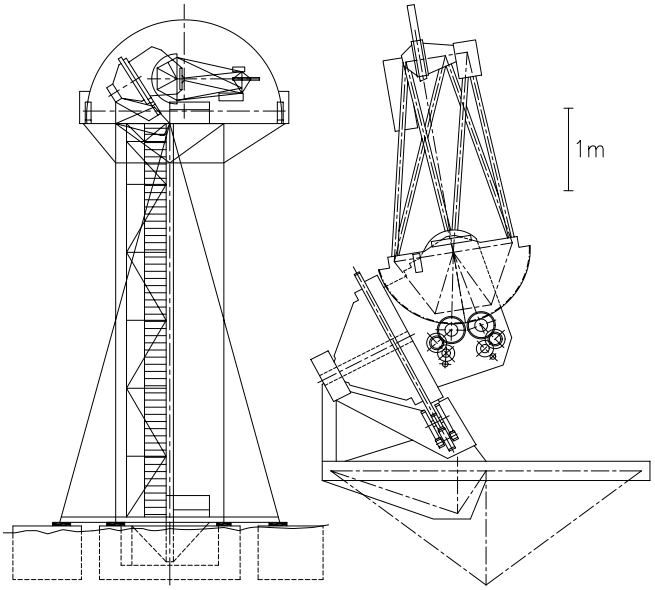

Fig. 4. Structural DOT sketches. North is to the right. Left, from the bottom up: foundation (four 2-m deep blocks of 25 m^3 concrete each); tower with two vertical leg triangles seen face-on, the other two edge-on; disconnected open-frame stairs and elevator; telescope in parked position; closed canopy. Right: telescope pointed at the sun at local noon on June 21. The parallactic mount consists of a full-circle hour-angle wheel (seen edge-on) and a half-circle declination wheel (face-on). A three times larger mirror than the present 45-cm primary can be accommodated (Sect. 7). The slender on-axis tube in the telescope top houses the prime-focus hardware and the G-band channel (Fig. 5). The remainder of the multi-wavelength imaging system and the focus monitor are housed to the left and the right of the incoming beam, respectively.

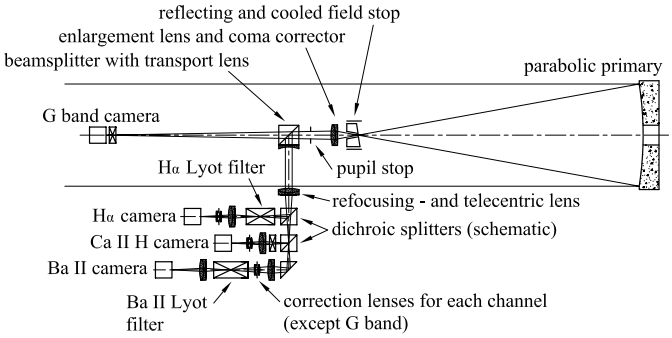

Fig. 5. Sketch of the DOT multi-wavelength re-imaging optics. The blue and red continua channels are omitted, the actual three-dimensional configuration differs considerably, and the actual dichroics are small-angle mirrors rather than cube splitters. Specific lens combinations are used at each wavelength to achieve diffraction-limited resolution with telecentric filter placement. See Bettonvil et al. (2003) for details.

Table 1. DOT filter specification.

designation	λ (Å)	width (Å)	type	tuning
blue continuum	4320	6	interference	fixed
red continuum	6540	3	interference	tiltable
G band	4305	10	interference	fixed
Ca II H	3968	1.35	interference	tiltable
Hα	6563	0.25	Lyot	tunable
Ba II	4554	0.08	Lyot	tunable

More detail on DOT design and hardware is given in Bettonvil et al. (2003).

on-axis. The latter begins with a field stop which passes only 1.6 mm or 3 arcmin of the primary image. The 200 W heat load in the remainder is removed through reflection and water cooling. In addition, air suction is applied around the field stop to avoid schlieren in the incoming beam.

Focus adjustment is required to compensate for thermal expansion of the top supports and also for flat-fielding. It is done by shifting the prime-focus field stop together with the enlargement lens and pupil stop behind it (Fig. 5). A precise phase-diverse focusing system continually monitors the granulation contrast in two image planes, using a video camera and frame grabber. Balancing the two contrasts maintains the location of the focal plane midway between the two samplings.

The DOT is protected against inclement weather by a 7-m diameter fold-away clamshell canopy, made of heavy PVC cloth mounted on heavy steel ribs. It opens nearly completely and is designed to be closeable in winds up to 30 m/s and to withstand hurricanes up to 70 m/s. Its teflon-like PVDF coating sheds snow and ice very well, so that the canopy remains remarkably free of ice loads (which commonly pose problems at the La Palma site). A 9-m copy is presently being constructed for GREGOR (`http://gregor.kis.uni-freiburg.de/`). The platform mesh floor is covered with removable wood panels during winter and during technical work on the telescope.

4. Multi-wavelength re-imaging

Figure 5 summarizes the DOT multi-wavelength re-imaging system schematically. Six channels feed six identical CCD cameras with concurrent co-spatial images through different filters specified in Table 1. Design detail is given by Bettonvil et al. (2003).

The motivation to select the six diagnostics listed in Table 1 is, respectively:

- G band: this dark feature (labeled G by Fraunhofer) is made up of CH lines and brightens considerably in magnetic elements, probably due to enhanced hot-wall visibility from molecular dissociation (Rutten et al. 2001b; Sánchez Almeida et al. 2001; Steiner et al. 2001; Langhans et al. 2002). It has become the preferred diagnostic to locate and follow small intergranular magnetic elements (e.g., Muller 1994; Title & Berger 1996; Berger et al. 1998a, 1998b; Berger & Title 2001).
- blue continuum: useful to disentangle granulation and magnetic bright points through differentiation with synchronous G-band images (van Ballegooijen et al. 1998).
- Ca II H: mapping the chromospheric network and internetwork oscillation patterns (Lites et al. 1999). At line center, resonance scattering causes intrinsic loss of resolution,

but we are nevertheless pleased by the sharpness of our initial speckle-restored Ca II H movies. The filter has a computer-controlled tiltable mount which permits precise passband calibration and tuning through the extended violet Ca II H wing to sample different heights in the upper photosphere, with straightforward interpretation thanks to the LTE character of Ca II H wing formation (cf. Ayres 1977) and the population dominance of the calcium ion ground state. This diagnostic also permits precise DOT movie co-registration with the very similar ultraviolet movies from TRACE (Rutten et al. 1999), an important asset to combine DOT Hα movies with TRACE EUV movies in, e.g., moss studies (De Pontieu et al. 1999).

– Hα: mapping low-lying loops complementary to EUV coronal loops as well as the footpoints of hot X-ray loops (Schrijver & Title 2002; De Pontieu 2003). Hα mottles and fibrils are likely to be partially optically thin, so that speckle reconstruction will yield considerable sharpness gain over older data. However, the narrow filter bandwidth requires multi-channel speckle restoration as developed by Keller & von der Lühe (1992), and the line formation complexity due to large Doppler modulation and NLTE control of both the line opacity and the line source function requires sophisticated data interpretation (e.g., Molowny-Horas et al. 1999). The Zeiss filter comes from the former Ottawa River Solar Observatory (Gaizauskas 1976).

– red continuum: primarily added to enable dual-channel Hα restoration, but of interest in itself as longer-wavelength sample of the low photosphere. The filter is actually an Hα interference filter in a computer-controlled tiltable mount which may also be used to sample the extended Hα absorption wing on the disk or to collect all Hα photons emitted at any Dopplershift by off-limb structures such as prominences (Stellmacher & Wiehr 2000).

– Ba II: a very promising mid-photosphere Doppler diagnostic due to its wide but boxy profile shape and large atomic mass (Sütterlin et al. 2001b). Two-channel reconstruction using the G-band and/or blue continuum images may be needed in view of the very narrow filter bandwidth. The tunable Lyot filter was built at the Irkutsk Institute of Solar-Terrestrial Physics (Kushtal & Skomorovsky 2002).

Together, these diagnostics provide tomography of the solar atmosphere sampling many heights. The blue continuum, close to the $\lambda = 4000$ Å opacity minimum, samples the photosphere slightly below the zero point of the standard height scale with $h = 0$ km at $\tau_{5000} = 1$. The G band samples fluxtubes even deeper. The red continuum is formed a few tens of km higher, with different Planck-function sensitivity to temperature fluctuations. The Ca II H wings sample heights throughout the whole photosphere depending on the filter setting, up to $h \approx 500$ km. Ca II H line center is sensitive to inhomogeneities up to double that height. The Ba II line samples Dopplershift in the middle photosphere. Hα originates as deep as the upper photosphere in very quiet regions, but may also sample fibrils and mottles far higher, up to multiple thousand km.

5. Speckle acquisition and reconstruction

The DOT employs Hitachi KP-F100 cameras with Sony ICX085 CCD chips, 1296×1030 px^2, pixel size 6.7 μm square, well depth 16 000 electrons, 10-bit readout, up to 12 f/s frame rate. Affordability dictated the selection of these machine-vision cameras, which pose linearity problems that must be corrected in the reduction. Their chip size, combined with the choice to have three samplings per angular resolution element (0.071 arcsec/px) limits the field to 92×73 arcsec^2. A few arcseconds are usually lost to image motion, residual solar rotation and guider flexure, differential refraction, active-region proper motion, and movie co-alignment. Each camera is connected through a dual 400-Mbps 100-m long optical fiber link to its own data-acquisition computer in the Swedish SST building.

During the test phase, the incoming speckle bursts (about 100 frames with exposures below 10 ms) were written to disks and then taped for subsequent off-line speckle reconstruction on the assorted DOT computers in the Swedish building. This processing is highly demanding and presents a severe bottleneck, increasingly falling behind with the installation of more channels and cameras – presently, we suffer a year's backlog. Fortunately, this problem will soon be remedied by the installation of a recently funded large-throughput speckle processor with over a hundred CPUs. It is designed to store all speckle bursts from a continuous eight-hour six-camera run (about 1.5 Terabyte) on disks and process them all overnight. Since speckle reconstruction effectively represents data compression by the number of frames per burst, the processed data from such a super-run will amount to only a few DVDs.

The extensive pre-processing encompasses dark subtraction and flat-field scaling, co-alignment of all the frames per burst, and field tessellation into isoplanatic subfields – about a thousand, each 4.5×4.5 arcsec^2, with considerable spatial overlap to facilitate later re-assembly. Each subfield is then co-aligned to a reference frame throughout the burst. This part of the processing is communication-limited, leading to hybrid distributed-parallel rather than straightforward Beowulf architecture for the new speckle processor (cf. Denker et al. 2001).

The actual speckle reconstruction parallelizes well. The DOT code stems from the one initiated at Göttingen by Kneer and de Boer. Improvements were added by Sütterlin at Göttingen and Utrecht; the code was recently ported from IDL to C and parallelized by de Wijn. It computes speckle transfer functions from atmospheric modeling using spectral-ratio Fried parameter evaluation and applies statistical bi-spectral phase estimation in speckle masking, as developed over the years by Weigelt, von der Lühe, de Boer, and others (e.g., Weigelt 1977; Weigelt & Wirnitzer 1983; Lohmann et al. 1983; Hofmann & Weigelt 1986; von der Lühe 1984, 1985; Pehlemann & von der Lühe 1989; de Boer 1993, 1995, 1996; Sütterlin & Wiehr 1998; see also Denker 1998 and references therein).

The code corrects for the asymmetrical DOT aperture obstruction and for camera non-linearity. The implementation of two-channel reconstruction following Keller & von der Lühe (1992) involved collaboration with K. Janssen at Göttingen.

The subsequent post-processing consists of subfield matching to the mean of the speckle burst, subfield re-assembly into

a full reconstructed image, image-to-image alignment to generate a movie per wavelength, and movie-to-movie co-alignment between wavelengths.

6. Open-DOT program

The imminent completion of DOT multi-wavelength imaging and high-volume speckle processing necessitates preparation for frequent observing, including DOT utilization by external colleagues and as partner in multi-telescope campaigns in an "open-DOT" program which we aim to start in 2004 and outline here.

The operation of the DOT is sufficiently complex that at least two of the authors must be present on site. It is impractical for a small university group as ours, with appreciable teaching duties in Utrecht, to man the DOT year-round. We therefore aim at frequent operation in service mode during the best-seeing season, and at campaign operation in common-user mode the rest of the year. The fortunate overlap between the good-seeing season (spring to autumn) and the academic summer recess will be exploited by bringing students to La Palma to assist in the observing.

Figure 3 suggests time allocation in one- to two-week slots to maximize the probability of collecting at least some high-resolution sequences per program. The scheduling and time allotment will involve a time allocation committee chaired by the first author. Since solar activity will decline the coming years, active-region programs will have priority, possibly in a bumping mode.

The actual DOT targeting will be flexible and may vary on short notice. A real-time link to the DOT control displays and incoming sample images will be supplied via the web. The DOT data product will consist of fully reduced and co-aligned multi-wavelength movies, on DVDs mailed soon after the observing.

It should be emphasized that, so far, all DOT data are public, and that we intend to continue this policy. A web-accessible inventory with compressed partial data sets, comparable to the MPEG movies on the present DOT website, will serve as quick-look search facility until integration into the upcoming world-wide Virtual Solar Observatory.

7. Future DOT

The present DOT tower, telescope mount and canopy permit aperture tripling from 45 cm to 140 cm without change (Fig. 4). Numerical simulations using artificial but realistic high-resolution data, kindly contributed by C.U. Keller of the National Solar Observatory in Tucson, indicate that low-order adaptive optics combined with speckle reconstruction will deliver full-field resolution near the corresponding 0.07 arcsec diffraction limit already at $r_0 \approx 10$ cm seeing. An appropriate optics design combining a new parabolic 140-cm primary with the present multi-wavelength re-imaging system in a new telescope top is available on the DOT website. This design includes flexible trade-off choice between pupil size and field size to match the ambient seeing optimally.

Our goal is to realize such a DOT upgrade by the time the Solar-B mission will provide 0.2-arcsec optical image streams from space.

8. Conclusion

Solar physics flourishes in a remarkable renaissance thanks to continuous high-cadence observing from space platforms, groundbased observing techniques that remove the degradation caused by seeing, and realistic numerical situations. These advances permit a fruitful and intrinsically necessary shift from static to time-dependent description: solar physics becomes a science of movies. Through its consistent speckle reconstruction over its whole field of observation, the DOT joins the sustained-quality type of digital movie making initiated with the SVST, SOHO, and TRACE. Specific research topics to which DOT movies will be suited are:

- network and internetwork oscillations, gravity waves, umbral flashes, wave pistoning, canopy wave penetration;
- fluxtube dynamics and patterns, magnetic carpet topology and evolution, sunspot structure and dynamics, active region emergence and decay, prominence stability and eruptions;
- moss structure and dynamics, spicule physics, tube-loop coupling.

We look forward to share these DOT capabilities with our colleagues abroad.

Acknowledgements. The DOT is operated by Utrecht University at the Spanish Observatorio del Roque de los Muchachos of the Instituto de Astrofísica de Canarias. The DOT control room is housed in the SST building of the Institute for Solar Physics of the Royal Swedish Academy of Sciences. We are much indebted to our SST colleagues for their hospitality, help, and frequent advice. The DOT is presently funded by Utrecht University, the Netherlands Organisation for Scientific Research NWO, the Netherlands Graduate School for Astronomy NOVA, and SOZOU. The DOT was built by the workshops of Utrecht University and the Central Workshop of Delft University of Technology with funding from Technology Foundation STW. The speckle data acquisition and re-imaging systems were built by the Instrumentele Groep Fysica at Utrecht. The Netherlands Foundation for Research in Astronomy ASTRON provides advice and facilities for optics testing. The DOT speckle processor is funded by NWO. Adaptation of the Göttingen speckle code was part of the EC–TMR European Solar Magnetometry Network ESMN. The present DOT efforts are part of the EC–RTN European Solar Magnetism Network under contract HPRN-CT-2002-00313. The Hα Lyot filter is on loan from the National Research Council Canada through V. Gaizauskas. The Ba II Lyot filter is on loan from the Institute of Solar-Terrestrial Physics at Irkutsk through V. I. Skomorovsky, with support from INTAS under Agreement 00-00084 and from the Pieter Langerhuizen Lambertuszoon Fonds. The scintillometer comes from the National Solar Observatory through J. M. Beckers. R. J. Rutten and A. G. de Wijn acknowledge travel support from the Leids Kerkhoven-Bosscha Fonds and hospitality at Montana State University in Bozeman.

References

Ayres, T. R. 1977, ApJ, 213, 296
Balthasar, H., Sütterlin, P., & Collados, M. 2001, Astron. Nachr., 322, 367
Beckers, J. M., & Rutten, R. J. 1998, New Astron. Rev., 42, 489
Berger, T. E., & Title, A. M. 2001, ApJ, 553, 449

Berger, T. E., Löfdahl, M. G., Shine, R. S., & Title, A. M. 1998a, ApJ, 495, 973
Berger, T. E., Löfdahl, M. G., Shine, R. S., & Title, A. M. 1998b, ApJ, 506, 439
Bettonvil, F. C. M., Hammerschlag, R. H., Sütterlin, P., Jägers, A. P., & Rutten, R. J. 2003, in Innovative Telescopes and Instrumentation for Solar Astrophysics, ed. S. L. Keil, & S. V. Avakyan, Proc. SPIE, 4853, 306
Brandt, P. N., & Righini, A. 1985, Vistas Astron., 28, 437
Brandt, P. N., & Wöhl, H. 1982, A&A, 109, 77
de Boer, C. R. 1993, Ph.D. Thesis, Göttingen
de Boer, C. R. 1995, A&AS, 114, 387
de Boer, C. R. 1996, A&AS, 120, 195
De Pontieu, B. 2003, in Turbulence, Waves and Instabilities in the Solar Plasma, ed. R. von Fay-Siebenbürgen, K. Petrovay, J.-L. Ballester, & M. Aschwanden, Proc. NATO ARW (Dordrecht: Kluwer), in press
De Pontieu, B., Berger, T. E., Schrijver, C. J., & Title, A. M. 1999, Sol. Phys., 190, 419
Denker, C. 1998, Sol. Phys., 180, 81
Denker, C., Yang, G., & Wang, H. 2001, Sol. Phys., 202, 63
Gaizauskas, V. 1976, JRAS Can., 70, 1
Hammerschlag, R. H. 1973, JOSO Annual Report, 85
Hammerschlag, R. H. 1981, in Solar Instrumentation: What's Next?, ed. R. B. Dunn, Proc. Sacramento Peak National Observatory Conference, Sunspot, New Mexico, 547
Hammerschlag, R. H. 1983, Proc. SPIE, 444, 138
Hammerschlag, R. H., & Bettonvil, F. C. M. 1998, New Astron. Rev., 42, 485
Hammerschlag, R. H., Jägers, A. P., & Bettonvil, F. C. M. 2003, in Innovative Telescopes and Instrumentation for Solar Astrophysics, ed. S. L. Keil, & S. V. Avakyan, Proc. SPIE, 4853, 294
Hoekzema, N. M., Brandt, P. N., & Rutten, R. J. 1998, A&A, 333, 322
Hofmann, K., & Weigelt, G. 1986, A&A, 167, L15
Keller, C. U., & von der Lühe, O. 1992, A&A, 261, 321
Kushtal, G. I., & Skomorovsky, V. I. 2002, Proc. SPIE, 4900, 504
Langhans, K., Schmidt, W., & Tritschler, A. 2002, A&A, 394, 1069
Lites, B. W., Rutten, R. J., & Berger, T. E. 1999, ApJ, 517, 1013
Lohmann, A. W., Weigelt, G., & Wirnitzer, B. 1983, Appl. Opt., 22, 4028
Lui, Z., & Beckers, J. M. 2001, Sol. Phys., 198, 197
Molowny-Horas, R., Heinzel, P., Mein, P., & Mein, N. 1999, A&A, 345, 618
Muller, R. 1994, in Solar Surface Magnetism, ed. R. J. Rutten, & C. J. Schrijver, NATO ASI Series C 433 (Dordrecht: Kluwer), 55
Nisenson, P., van Ballegooijen, A. A., de Wijn, A. G., & Sütterlin, P. 2003, ApJ, 587, 458
Pehlemann, E., & von der Lühe, O. 1989, A&A, 216, 337
Rouppe van der Voort, L. H. M., Rutten, R. J., Sütterlin, P., Sloover, P. J., & Krijger, J. M. 2003, A&A, 403, 277
Rutten, R. J. 1999, in High Resolution Solar Physics: Theory, Observations, and Techniques, ed. T. R. Rimmele, K. S. Balasubramaniam, & R. R. Radick, Proc. 19th NSO/Sacramento Peak Summer Workshop, ASP Conf. Ser., 183, 147
Rutten, R. J. 2003, in Astronomy with Small Telescopes in the Era of Large Telescopes, ed. T. Oswalt (Dordrecht: Kluwer), in press
Rutten, R. J., De Pontieu, B., & Lites, B. W. 1999, in High Resolution Solar Physics: Theory, Observations, and Techniques, ed. T. R. Rimmele, K. S. Balasubramaniam, & R. R. Radick, Proc. 19th NSO/Sacramento Peak Summer Workshop, ASP Conf. Ser., 183, 383
Rutten, R. J., Hammerschlag, R. H., Sütterlin, P., & Bettonvil, F. C. M. 2001a, in Advanced Solar Polarimetry – Theory, Observation, and Instrumentation, ed. M. Sigwarth, Proc. 20th NSO/SP Summer Workshop, ASP Conf. Ser., 236, 25
Rutten, R. J., Kiselman, D., Rouppe van der Voort, L., & Plez, B. 2001b, in Advanced Solar Polarimetry – Theory, Observation, and Instrumentation, ed. M. Sigwarth, Proc. 20th NSO/SP Summer Workshop, ASP Conf. Ser., 236, 445
Sánchez Almeida, J., Asensio Ramos, A., Trujillo Bueno, J., & Cernicharo, J. 2001, ApJ, 555, 978
Schrijver, C. J., & Title, A. M. 2002, Sol. Phys., 207, 223
Simon, G. W., Brandt, P. N., November, L. J., Scharmer, G. B., & Shine, R. A. 1994, in Solar Surface Magnetism, ed. R. J. Rutten, & C. J. Schrijver, NATO ASI Series C 433 (Dordrecht: Kluwer), 261
Sobotka, M., & Sütterlin, P. 2001, A&A, 380, 714
Steiner, O., Hauschildt, P. H., & Bruls, J. 2001, A&A, 372, L13
Stellmacher, G., & Wiehr, E. 2000, Sol. Phys., 196, 357
Sütterlin, P., & Wiehr, E. 1998, A&A, 336, 367
Sütterlin, P. 2001, A&A, 374, 21
Sütterlin, P., Hammerschlag, R. H., Bettonvil, F. C. M., et al. 2001a, in Advanced Solar Polarimetry – Theory, Observation, and Instrumentation, ed. M. Sigwarth, Proc. 20th NSO/SP Summer Workshop, ASP Conf. Ser., 236, 431
Sütterlin, P., Rutten, R. J., & Skomorovsky, V. I. 2001b, A&A, 378, 251
Title, A. M., & Berger, T. E. 1996, ApJ, 463, 797
van Ballegooijen, A. A., Nisenson, P., Noyes, R. W., et al. 1998, ApJ, 509, 435
von der Lühe, O. 1984, J. Opt. Soc. Am., 1, 510
van Ballegooijen, A. A., Nisenson, P., Noyes, R. W., et al. 1985, A&A, 150, 229
Weigelt, G., & Wirnitzer, B. 1983, Opt. Lett., 8, 389
Weigelt, G. P. 1977, Opt. Comm., 21, 55